

Dedicated to Professor Ioan-Iovitz Popescu's 80th Anniversary

SPATIAL SOLITONS IN PARITY-TIME-SYMMETRIC MIXED LINEAR-NONLINEAR OPTICAL LATTICES: RECENT THEORETICAL RESULTS

YINGJI HE^{1,*}, DUMITRU MIHALACHE^{2,**}

¹ Guangdong Polytechnic Normal University, School of Electronics and Information, 510665
Guangzhou, China

² “Horia Hulubei” National Institute for Physics and Nuclear Engineering, 077125 Magurele-
Bucharest, Romania

* E-mail: heyingji8@126.com; **E-mail: Dumitru.Mihalache@nipne.ro

Received July 31, 2012

Abstract. We provide a brief review of recent theoretical studies of optical spatial solitons in parity-time- (PT-) symmetric mixed linear-nonlinear lattices. The existence and stability of optical spatial solitons forming in PT-symmetric lattices with spatially periodic modulation of the Kerr nonlinearity are briefly overviewed. The linear optical lattices are considered to be either regular lattices or superlattices formed by the superposition of two periodic lattice potentials having commensurable lattice periods. The obtained results show that different kinds of linear optical lattices can profoundly affect soliton properties. In particular, by mixing linear and nonlinear optical lattices, a lot of unique spatial soliton properties were put forward. These features may find potential applications in all-optical signal processing and in high-speed circuits for optical communications systems.

Key words: PT-symmetric optical lattices, optical spatial solitons, nonlinearity modulation.

1. INTRODUCTION

In 1998, Bender and Boettcher found in a seminal work [1] that non-Hermitian Hamiltonians can still have entirely real eigenvalue spectra provided that these Hamiltonians obey parity-time (PT) symmetry. Such types of Hamiltonians can also undergo a “phase transition” above a critical threshold, *i.e.*, a *spontaneous PT-symmetry-breaking*; above such transition point the eigenvalue spectrum ceases being entirely real-valued and becomes partially complex-valued [2–6].

In general, the action of the parity operator \mathbf{P} is defined by the relations $p \rightarrow -p$ and $x \rightarrow -x$ (here p and x are the momentum and position operators, respectively), while that of the time operator \mathbf{T} by the relations $p \rightarrow -p$, $x \rightarrow x$, and the complex conjugation $i \rightarrow -i$. Given the fact that the action of the time operator \mathbf{T} leads to

time reversal, i.e., $\mathbf{TH} = p^2/2 + V^*(x)$ (here \mathbf{H} is the Hamiltonian of the system), one gets $\mathbf{HPT} = p^2/2 + V(x)$ and $\mathbf{PTH} = p^2/2 + V^*(-x)$.

Thus one can conclude that a necessary condition for the Hamiltonian to be PT-symmetric is that the potential function $V(x)$ should fulfill the condition $V(x) = V^*(-x)$ [1, 7–8]. Therefore, the real part of the PT-symmetric complex-valued potential must be an even function of the position variable x , whereas the imaginary part should be an odd function of the spatial variable x . The PT-symmetric potentials can be realized through using the complex refractive index distribution $n(x) = n_0 + n_R(x) + in_I(x)$, where n_0 represents the background refractive index and x is the normalized transverse coordinate [7–9]. Thus, to satisfy the PT-symmetry condition, $n_R(x)$ must be an even function of the transverse spatial coordinate x , while the gain (or loss) component $n_I(x)$ of the refractive index distribution $n(x)$ should be an odd one.

Beam dynamics in PT-symmetric complex-valued periodic optical lattices can exhibit unique characteristics, such as double refraction, power oscillations, nonreciprocal diffraction patterns, etc. In the theoretical arena, it was studied the effect of Kerr nonlinearity on the unique beam dynamics in PT-symmetric complex-valued periodic optical potentials, i.e., the formation of nonlinear self-trapped modes, alias *spatial solitons* in both one-dimensional (1D) and two-dimensional (2D) PT-symmetric synthetic linear optical lattices (OLs) [7, 8, 10].

Defect modes in PT-symmetric periodic complex-valued potentials have also been studied [11, 12]. *Gap solitons* in parity-time complex-valued periodic OLs with the real part of the linear lattice potential having the shape of a double-periodic function (a superlattice potential) were investigated in Ref. [13]. Stable 1D and 2D bright spatial solitons in defocusing Kerr media with PT-symmetric potentials have been found, too [14]. Also, it has been found that the gray solitons in PT-symmetric potentials can be stable [15].

Very recently, Nixon *et al.* systematically studied the stability properties of solitons in PT-symmetric lattices and found that both 1D and 2D solitons can propagate stably under appropriate conditions [16]. Two-dimensional solitons in PT-symmetric lattice potentials have been studied in a separate work by Zeng and Lan [17]. It was found in Ref. [17] that 2D gap solitons in the case of self-focusing nonlinearity may exist in PT-symmetric lattices, but they were found to be unstable due to unavoidable collapse instability.

Achilleos *et al.* [18] considered nonlinear analogs of PT-symmetric linear systems exhibiting defocusing nonlinearities. They studied both the ground state and odd excited states (dark solitons and vortices) of the system and they put forward the unique features of PT-symmetric systems exhibiting self-defocusing nonlinearities [18].

Based on multi-waveguides of PT-symmetric lattices, the coupled solitons can produce some new and intriguing phenomena. In a seminal recent work by Zezyulin and Konotop [19] nonlinear modes in finite-dimensional PT-symmetric systems were considered in detail. It was shown in Ref. [19] that the

transformations among PT-symmetric systems by rearrangements of waveguide arrays with gain and loss do not affect their pure real linear spectra; however, the nonlinear features of such PT-symmetric systems undergo significant changes.

Alexeeva *et al.* [20] studied spatial and temporal solitons in the PT-symmetric coupler with gain in one waveguide and loss in the other. It was shown in Ref. [20] that stability properties of both high- and low-frequency solitons are completely determined by a single combination of the soliton's amplitude and the gain-loss coefficient of the coupled waveguides. Moreover, in a recent paper by Chen *et al.* [21], optical modes in PT-symmetric double-channel waveguides have been reported, too.

Bragg gap solitons in PT-symmetric lattices with competing optical nonlinearities of the cubic-quintic type have been also investigated in a recent study [22]. These solitons were found to be unstable; however off-site gap solitons were found to be more robust than in-site gap solitons, see Ref. [22] for more details of this study. Various families of solitons (including multi-stable solitons) with even and odd geometrical symmetries are found in both the semi-infinite and the first gaps [23].

Recently, *nonlocal* optical nonlinearity has been introduced into the study of different models of PT-symmetric complex-valued potentials. For example, defect solitons in PT-symmetric potentials with nonlocal nonlinearity were investigated in a recent work by Hu *et al.* [24]. It was shown in Ref. [24] that for positive or zero defects, fundamental and dipole solitons can exist stably in the semi-infinite gap and the first gap, respectively. However, for negative defects, fundamental solitons can be stable in both the semi-infinite gap and the first gap, whereas dipole solitons were found to be unstable in the first gap, see Ref. [24]. It was also shown in Ref. [24] that when the modulation depth of the PT-symmetric optical lattices is small, defect solitons can be stable for both positive and zero defects, even if the PT-symmetric potential is above the phase transition point.

Yin *et al.* [25] in a recent study of solitons in PT-symmetric potentials with spatially modulated nonlocal nonlinearity revealed that the amplitude of the spatially modulated nonlinearity and the degree of the uniform nonlocality can profoundly affect the stability properties of solitons. There exist stable solitons in low-power region, and unstable ones in high-power region. In the unstable cases, the solitons exhibit jump from the original site (channel) to the next one, and they can continue the motion into the other adjacent channels, see Ref. [25]. Moreover, when the amplitude of the imaginary part of the linear PT-symmetric lattice exceeds a critical value (the so-called “phase transition” point), the lattice solitons were found to be unstable and to decay quickly upon propagation, see Ref. [25] for a detailed study of this issue.

The truncation of PT-symmetric complex-valued potentials breaks their symmetry and prohibits the formation of stationary states, at least around the edge of potential profile. This is different from the case of real-valued potentials. In the latter case, surface solitons that may form at the edge of truncated periodic lattices were theoretically studied and subsequently observed in one- and two-dimensional

settings, in both self-focusing and self-defocusing optical media [26]. Another interesting class of complex-valued potentials is represented by structures where linear gain acts only in one or several localized spots, while the real part of potential may be a periodic function. Such complex-valued potentials support dissipative solitons if additional nonlinear losses compensate localized gain [27–30]. Notice that in sharp contrast to PT-symmetric structures the truncation of such potentials still allows existence of stationary states even around the edge of potential if gain also acts around its edge [31]. Recently, it was revealed that truncated periodic complex potentials with homogeneous losses can support stable surface solitons in both focusing and defocusing media [32].

The study of solitons in nonlinear OLs has attracted a lot of attention; see a recent comprehensive review in this area [33]. Such nonlinear OLs represent a spatially periodic modulation of the local strength and sign of the optical nonlinearity. It should be mentioned that PT-symmetric nonlinear OLs can also support stable discrete solitons [34]. A series of incentive works in the area of PT-symmetric nonlinear lattices in various physical settings have been recently published [35–37]. The existence of localized modes, including multipole solitons, supported by PT-symmetric nonlinear lattices was recently reported [35]. Such PT-symmetric nonlinear OLs can be implemented by means of proper periodic modulation of nonlinear gain and losses, in specially engineered nonlinear optical waveguides.

Driben and Malomed [38] investigated in detail the problem of stability of solitons in PT-symmetric nonlinear optical couplers and reported families of analytical solutions for both symmetric and antisymmetric solitons in dual-core systems with Kerr nonlinearity and PT-balanced gain and loss. Also, stabilization of solitons in PT models with “supersymmetry” by periodic management in a system based on dual-core nonlinear waveguides with balanced gain and loss acting separately in the cores was investigated in Ref. [39].

Solitons in periodic mixed lattices with linear and nonlinear counterparts have been investigated, too. The issue of competition between the lattices of the linear and nonlinear types was first investigated by Bludov and Konotop [40] in the context of matter waves in Bose-Einstein condensates (BECs); see also a subsequent work [41] on gap solitons in BECs loaded in mixed linear-nonlinear optical lattices. Further, solitons in purely PT-symmetric nonlinear lattices [35, 42, 43], and solitons in mixed PT-symmetric linear-nonlinear lattices have been investigated, too [44]. It was found that the combination (superposition) of PT-symmetric linear and nonlinear lattices can stabilize lattice solitons and it was revealed that the parameters of the linear lattice periodic potential play a significant role in controlling the extent of the stability domains [44].

The present work briefly summarizes the recent theoretical studies of lattice solitons in PT-symmetric lattices with/without spatially periodic modulation of the Kerr-type nonlinearity. In the next section we briefly overview the most general model of spatial soliton propagation for self-focusing Kerr nonlinearities. In Sec. 3 we briefly review the results obtained so far for gap solitons forming in PT-

symmetric complex-valued periodic optical lattices with the real part of the linear lattice potential having the shape of a double-periodic function with commensurable periods, i.e., the typical case of a superlattice potential. The existence and stability of lattice solitons in PT-symmetric mixed linear-nonlinear optical lattices in self-focusing Kerr media are briefly discussed in Sec. 4. Solitons in PT-symmetric optical lattices with spatially periodic modulation of nonlinearity is briefly overviewed in Sec. 5. Finally, in Sec. 6 we summarize the results and we indicate a few possible extensions of these studies to other relevant physical settings.

2. THE MOST GENERAL MODEL

Spatial beam propagation in PT-symmetric periodic OLs with/without periodic modulation of the Kerr optical nonlinearity obeys the following normalized 1D nonlinear Schrödinger equation [7,44]:

$$i \frac{\partial q}{\partial z} + \frac{1}{2} \frac{\partial^2 q}{\partial x^2} + [v(x) + iw(x)]q + [1 - N(x)]|q|^2 q = 0, \quad (1)$$

where i is the imaginary unit, q is the complex field amplitude, and z and x are the normalized longitudinal coordinate and transverse coordinate, respectively. Note that in Eq. (1), $v(x)$ is an even function of transverse spatial coordinate x and $w(x)$ is an odd function; the nonlinear modulation function is $N(x)$; when $N(x) = 0$ the nonlinear modulation of the self-focusing Kerr nonlinearity is absent. The stationary solutions of Eq. (1) to be searched for are of the form $q(x,z) = f(x) \exp(i\mu z)$; here $f(x)$ is a complex-valued function, and μ is the corresponding propagation constant. Therefore, the complex-valued function $f(x)$ satisfies the following nonlinear differential equation:

$$\frac{1}{2} \frac{d^2 f}{dx^2} + [v(x) + iw(x)]f + [1 - N(x)]|f|^2 f = \mu f. \quad (2)$$

By substituting $f(x) = h(x) + ie(x)$ to Eq. (2), we obtain the two coupled nonlinear differential equations

$$\frac{1}{2} h_{xx} + vh - we + [1 - N(x)]e^2 h + [1 - N(x)]h^3 = \mu h, \quad (3a)$$

$$\frac{1}{2} e_{xx} + ve + wh + [1 - N(x)]h^2 e + [1 - N(x)]e^3 = \mu e, \quad (3b)$$

where h and e are real functions. In order to analyze the linear stability of stationary soliton solutions, we add the small perturbations $g(x)$ and $t(x)$ to the stationary soliton solution:

$$q(x, z) = \exp(i\mu z) \{ f(x) + [g(x) - t(x)] \exp(\delta z) + [g(x) + t(x)]^* \exp(\delta^* z) \},$$

see, e.g., Ref. [45]. Here, $g(x)$, $t(x) \ll 1$, and the superscript $*$ represents complex conjugation.

Next by substituting $q(x, z)$ to Eq. (1) and linearizing it, we get the following coupled nonlinear equations:

$$\begin{cases} \delta g = -i \left\{ \frac{d^2 t}{dx^2} - \mu t + \nu t - i w g + 2[1 - N(x)] \left[|f|^2 t - \frac{1}{4}(f^2 - f^{*2})g - \frac{1}{4}(f^2 + f^{*2})t \right] \right\}, \\ \delta t = -i \left\{ \frac{d^2 g}{dx^2} - \mu g + \nu g - i w t + 2[1 - N(x)] \left[|f|^2 g + \frac{1}{4}(f^2 + f^{*2})g + \frac{1}{4}(f^2 - f^{*2})t \right] \right\}. \end{cases} \quad (4)$$

The coupled equations (4) can be numerically solved by matrix eigenvalue method [45]. If $\text{Re}(\delta) > 0$, the solitons are linearly unstable, otherwise, they are stable.

The linear version of nonlinear differential equation (2) is

$$\frac{1}{2} \frac{d^2 f}{dx^2} + [v(x) + iw(x)]f = \mu f, \quad (5)$$

where, μ represents the propagation constant. According to Bloch theorem, the eigenfunctions of Eq. (5) are of the form $f = F_k \exp(ikx)$, where k is the Bloch wave number, and F_k is a periodic function of x with the same period as the functions $v(x)$ and $w(x)$.

Substituting the Bloch solution to Eq. (5), we can get the eigenvalue equation

$$\left(\frac{d^2}{dx^2} + 2ik \frac{d}{dx} - k^2 \right) F_k + [v(x) + iw(x)]F_k = \mu F_k. \quad (6)$$

The total soliton power P is defined as

$$P = \int_{-\infty}^{+\infty} |f|^2 dx.$$

The robustness of the spatial soliton propagation was tested in direct numerical simulations of Eq. (1) by adding a random noise (10% of the soliton amplitude) to the input soliton profile.

3. GAP SOLITONS IN PT-SYMMETRIC PERIODIC OLs WITH DOUBLE PERIODIC REAL PART OF LINEAR LATTICE POTENTIAL

Recently Zhu *et al.* [13] reported the existence and stability of *gap solitons* in PT-symmetric complex-valued periodic lattice potentials in the special case when

the real part of the linear periodic lattice potential is a superposition of two terms with commensurable periods (a superlattice potential). Thus in Eq. (1), the real part of the linear periodic lattice potential is a superposition of two periodic terms, $v(x) = \varepsilon \sin^2(x + \pi/2) + (1 - \varepsilon) \sin^2[2(x + \pi/2)]$, here ε is the parameter that controls the relative strength of the two periodic terms in the real part of the potential (superlattice part of the potential). Note that for the specific case studied in Ref. [13], the ratio of the two periods of the superlattice potential has been chosen to be 1/2. The imaginary part was $w(x) = \omega_0 \sin(2x)$ and the Kerr nonlinearity was uniform, i.e., $N(x) = 0$. The relative strength ε of the real part of the superlattice potential and the amplitude ω_0 of the imaginary part of the lattice potential significantly affect the stability features of solitons. In Ref. [13], the Eqs. (3a) and (3b) were numerically solved by the modified squared-operator method [46]. Equation (2) was numerically solved by the spectral renormalization method [47], in order to obtain soliton profiles.

The results shown in Figs. 1(a) and 1(b) indicate that when $\varepsilon = 0.3$ and $\omega_0 = 0.1$, the solitons exist in the semi-infinite gap and can stably propagate in the low power region. The field profiles and propagation dynamics corresponding to two typical stable cases for $\mu = 0.55$ and $\mu = 1.4$ are shown in Figs. 2a,d and 2(b,e), respectively. In the high power region, solitons were found to be unstable. For $\mu = 1.8$, periodic oscillations of soliton power occur, as shown in Fig. 2(f). Note that when $\omega_0 = 0.1$, the stability features will vary for different values of ε . For $\varepsilon = 0.7$, the band diagram is also a real-valued one and the soliton is stable at $\mu = 3$, as shown in Fig. 2k. In the case of $\mu = 3$, the solitons were found to be unstable for both $\varepsilon = 0.2$ and $\varepsilon = 0.3$. When $\varepsilon = 0.2$, the band diagram is partially a complex-valued one, and the PT-symmetry is spontaneously broken. Figure 2l shows the instability at $\mu = 1.3$ and $\varepsilon = 0.2$. However, for the same value of μ , the gap solitons were found to be stable at $\varepsilon = 0.3$ and $\varepsilon = 0.7$, see Ref. [13] for a detailed discussion of these issues.

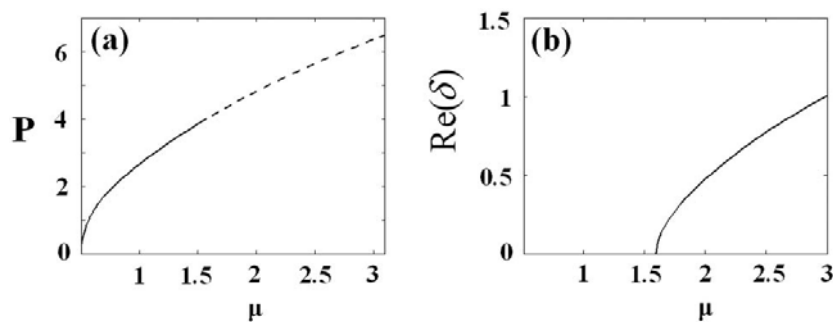


Fig. 1 – For $\varepsilon = 0.3$ and $\omega_0 = 0.1$: a) power P versus μ (the solid curve represents the stable region and the dashed curve represents the unstable region); b) $\text{Re}(\delta)$ versus μ ; after Ref. [13].

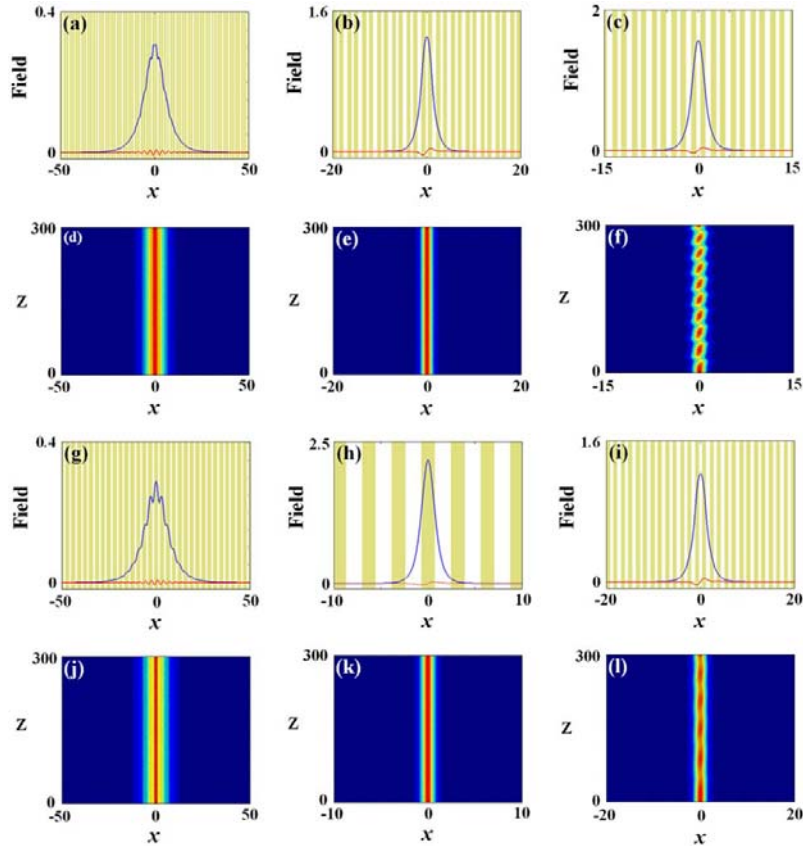


Fig. 2 – Soliton profile (the blue curve is the real part and the red curve is the imaginary part) and soliton propagation for $\omega_0 = 0.1$: a, d) $\mu = 0.55$ and $\varepsilon = 0.3$; b, e) $\mu = 1.4$ and $\varepsilon = 0.3$; c, f) $\mu = 1.8$ and $\varepsilon = 0.3$; g, j) $\mu = 0.55$ and $\varepsilon = 0.7$; h, k) $\mu = 3$ and $\varepsilon = 0.7$; i, l) $\mu = 1.3$ and $\varepsilon = 0.2$; after Ref. [13].

4. SOLITONS IN PT-SYMMETRIC MIXED LINEAR-NONLINEAR OLS

A. *The study of the general case when the PT-symmetric linear lattice potential is different from the PT-symmetric nonlinear lattice potential.* As in Ref. [44], we consider in Eq. (1), that the PT-symmetric linear lattice profile is given by the periodic functions $v(x) = \varepsilon_0 \cos^2(x)$ and $w(x) = \omega_0 \sin(2x)$, whereas the PT-symmetric nonlinear lattice modulation is given by $N(x) = v_1(x) + w_1(x)$. Here $v_1(x) = \varepsilon_1 \cos(2x)$ and $w_1(x) = -\omega_1 \sin(2x)$. The amplitudes ε_0 and ω_0 are the amplitudes of real and imaginary parts of the linear OLS, respectively, and the amplitudes ε_1 and ω_1 are the nonlinearity modulation coefficients. Thus in the most general case to be briefly overviewed in this subsection we take different periodic spatial distributions, i.e., we consider different linear and nonlinear lattice potentials.

Therefore for the above choice of the two jointly acting linear and nonlinear lattice potentials, the real parts, the sign of the imaginary parts, and the amplitudes of the modulation profiles are totally different, see Ref. [44].

First, we fix the parameters ε_0 and ω_0 of the PT symmetric linear lattice in order to investigate the effect of PT-symmetric nonlinear lattices on soliton propagation [44]. We then fix the values of the two parameters describing the PT-symmetric linear OLs as $\varepsilon_0 = 4$ and $\omega_0 = 0.8$. The dependences of soliton power P on propagation constant μ are shown in Figs. 3a, 3b, and 3c, for three sets of nonlinear OL parameters $\varepsilon_1 = 0.1$ and $\omega_1 = 0.1$, $\varepsilon_1 = 0.5$ and $\omega_1 = 0.5$, and $\varepsilon_1 = 1$ and $\omega_1 = 1$, respectively. From Fig. 3, we see that the soliton power increases with the decrease of the amplitudes ε_1 and ω_1 of the nonlinearity modulation. This can be explained as follows. Because we are considering here a self-focusing Kerr nonlinearity, if the depth of nonlinear lattice increases, the corresponding self-focusing effect exerted on the optical beam, which is determined by $[1 + \nu_1(x)]|q|^2 q$ and the associated nonlinear gain effect coming from the imaginary part of the nonlinear lattice potential are becoming stronger. In addition, for a certain depth of the nonlinear lattice, a higher power (or peak amplitude) of solitons will also cause a much stronger self-focusing effect on the optical beam. If the combination of self-focusing and nonlinear gain effects is stronger than a certain critical limit, the lattice solitons will collapse. So the existence of solitons in our specific situation requires that their peak amplitudes (or powers) must decrease with increase of the depth of nonlinear lattice in order to avoid the destruction of the solitons during propagation due to the presence of a very high self-focusing effect. Note that if only the depth of dissipative part of nonlinearity modulation is increased, the soliton power still decreases, i.e., the effect of the imaginary (dissipative) part of nonlinearity modulation on the soliton power is smaller than that induced by the real part of the nonlinearity modulation, see Ref. [44] for more details of these studies.

Further we consider the longitudinal evolution of lattice solitons. The results of simulations are shown in Fig. 4 where both the soliton field profiles and their corresponding evolutions during propagation were plotted. We can see that the stable soliton regions are as follows: $2.7 \leq \mu \leq 3.4$ for $\varepsilon_1 = 0.1$ and $\omega_1 = 0.1$, $2.7 \leq \mu \leq 3.2$ for $\varepsilon_1 = 0.5$ and $\omega_1 = 0.5$, and $2.7 \leq \mu \leq 3.0$ for $\varepsilon_1 = 1$ and $\omega_1 = 1$. These results clearly show that lattice solitons can only stabilize in the low power range and that the stable soliton domain narrows with the growth of the amplitudes ε_1 and ω_1 of nonlinear lattices, see Ref. [44].

Typical stable soliton evolutions for the propagation constant $\mu = 2.7$ are plotted in Figs. 4a, b for $\varepsilon_1 = 0.1$ and $\omega_1 = 0.1$, Figs. 4e, f for $\varepsilon_1 = 0.5$ and $\omega_1 = 0.5$, and Figs. 4i, j for $\varepsilon_1 = 1$ and $\omega_1 = 1$, while typical unstable soliton evolutions for $\mu = 5$ are given in Figs. 4c, d for $\varepsilon_1 = 0.1$ and $\omega_1 = 0.1$, Figs. 4g, h for $\varepsilon_1 = 0.5$ and $\omega_1 = 0.5$, and Figs. 4k, l for $\varepsilon_1 = 1$ and $\omega_1 = 1$ [44].

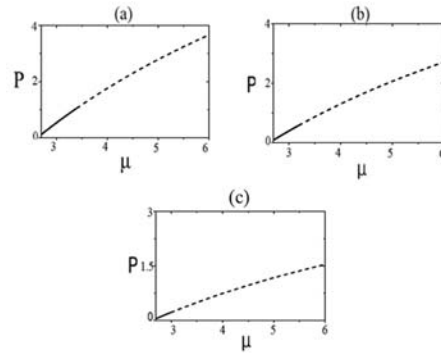


Fig. 3 – Power P versus propagation constant μ for $\varepsilon_0 = 4$ and $\omega_0 = 0.8$ and: a) $\varepsilon_1 = 0.1$ and $\omega_1 = 0.1$; b) $\varepsilon_1 = 0.5$ and $\omega_1 = 0.5$; c) $\varepsilon_1 = 1$ and $\omega_1 = 1$. The stable branches are plotted by solid curves and the unstable branches are plotted by dashed curves; after Ref. [44].

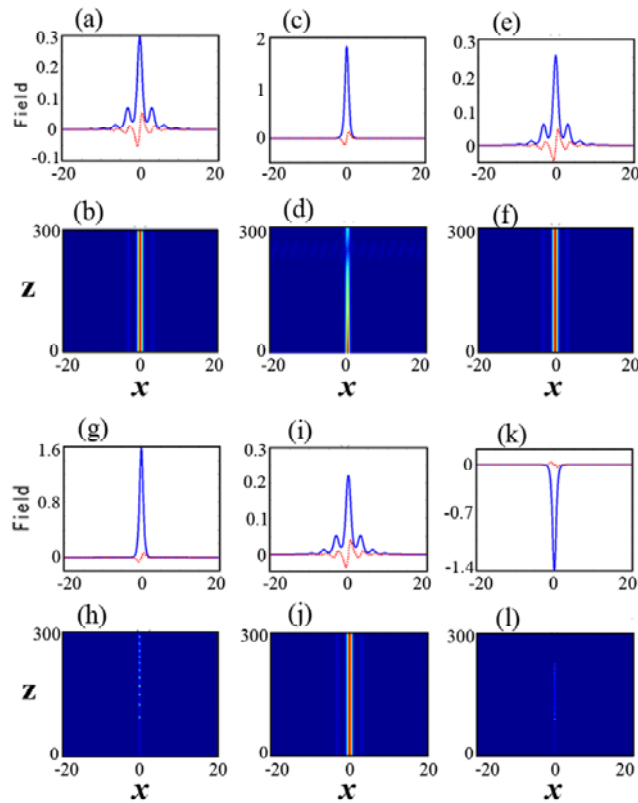


Fig. 4 – Soliton profiles (the solid curves show the real parts and the dotted curves show the corresponding imaginary parts) and soliton evolution for $\varepsilon_0 = 4$ and $\omega_0 = 0.8$. Stable soliton evolutions for $\mu = 2.7$: a, b) for $\varepsilon_1 = 0.1$ and $\omega_1 = 0.1$; e, f) for $\varepsilon_1 = 0.5$ and $\omega_1 = 0.5$; i, j) for $\varepsilon_1 = 1$ and $\omega_1 = 1$. Unstable soliton evolutions for $\mu = 5$: c, d) for $\varepsilon_1 = 0.1$ and $\omega_1 = 0.1$; g, h) for $\varepsilon_1 = 0.5$ and $\omega_1 = 0.5$; k, l) for $\varepsilon_1 = 1$ and $\omega_1 = 1$; after Ref. [44].

B. The study of a special case when the PT-symmetric linear lattice potential is identical with the PT-symmetric nonlinear lattice potential. In what follows we discuss the special case when we consider identical PT-symmetric lattice potentials for both linear and nonlinear OLs, see Ref. [44] for a detailed study of this issue. We thus take the following modulation profiles: $v(x) = \varepsilon_0 \cos^2(x)$, $w(x) = \omega_0 \sin(2x)$, $v_1(x) = v(x)$, and $w_1(x) = w(x)$.

In order to find out the effect of modification of the amplitudes of the real and imaginary parts of the linear and nonlinear modulation profiles, on soliton propagation, we select three typical sets of parameters: (i) $\varepsilon_0 = 4$ and $\omega_0 = 0.8$, (ii) $\varepsilon_0 = 3$ and $\omega_0 = 0.8$, and (iii) $\varepsilon_0 = 4$ and $\omega_0 = 0.6$. The corresponding total powers P versus propagation constant μ are shown in Fig. 5. The stability domains are found to be $2.7 \leq \mu \leq 3.5$, $1.9 \leq \mu \leq 3.0$, and $2.7 \leq \mu \leq 4.5$, for the above sets of parameters (i), (ii), and (iii), respectively. These results clearly show that solitons can be stable only in the low power regimes and that the soliton stability region increases with the decrease of the amplitudes of imaginary parts of modulation profiles of both kinds of OLs. Also, soliton stability region shifts towards the lower values of μ with the decrease of the amplitude of modulation profiles of real parts of both kinds of OLs. We thus conclude that the parameters of PT symmetric linear lattices play an important role in controlling the magnitude of soliton stability region.

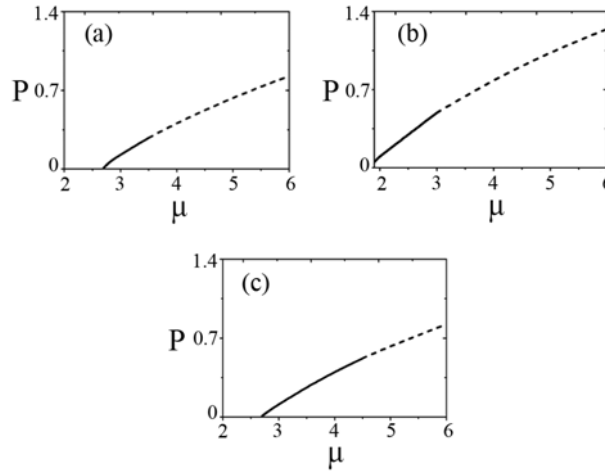


Fig. 5 – Power P versus μ for: a) $\varepsilon_0 = 4$ and $\omega_0 = 0.8$; b) $\varepsilon_0 = 3$ and $\omega_0 = 0.8$; c) $\varepsilon_0 = 4$ and $\omega_0 = 0.6$. The stable regions are plotted by solid curves and the unstable regions are plotted by dashed curves; after Ref. [44].

We conclude this subsection by noting that the lattice solitons are tightly bound by the mixed PT-symmetric linear-nonlinear lattice; the high-amplitude

solitons are compacted within one spatial lattice period, which is equal to π in all numerical simulations. The most unstable solitons experience a fast decay of energy upon propagation, whereas the less unstable ones exhibit slight oscillations of their peak amplitudes. The results reported in Ref. [44] can be extended in the direction of considering in detail the competition between linear and nonlinear lattice potentials, i.e., by choosing different gain/loss combinations of the dissipative parts of both linear and nonlinear lattice potentials.

5. SOLITONS IN PT-SYMMETRIC OLs WITH SPATIAL PERIODIC MODULATION OF NONLINEARITY

Recently, He *et al.* [43] reported a detailed study of optical spatial solitons in PT-symmetric lattices with spatially periodic modulation of Kerr nonlinearity. In what follows, we briefly overview the results reported by He *et al.* [43]. Thus in Eq. (1), we select $w(x) = \omega_0 \sin(2x)$, $v(x) = \varepsilon \cos^2(x)$, and the nonlinear modulation function is given by $N(x) = p \cos^2(x/T)$; here p is the amplitude of the modulation of the nonlinear refractive index and $\pi \times T$ is the corresponding period. The numerical results for power P versus μ and for $\text{Re}(\delta)$ versus μ are shown in Fig. 6 for different depths p of the nonlinear modulation function $N(x)$. Figure 6a shows that for $\varepsilon = 4$ and $\omega_0 = 0.8$, the solitons existing in the semi-infinite gap can stably propagate in the low power regime. Moreover, we see from the numerical values of $\text{Re}(\delta)$ shown in Fig. 6b, that the stable range of soliton propagation increases with the decrease of the depth p of the modulation function $N(x)$. When $p > 1$, the nonlinearity becomes a defocusing one. In this case, the salient features of solitons are similar to those for a focusing nonlinearity, including power increase with propagation constant and stable solitons existing in low power domain, while unstable ones in high power domain. If the parameter p further grows, the region of stable solitons decreases, and above some critical value of p , there are no stable localized modes. A typical example of these results can be seen in Fig. 6 for $p = 1.2$ corresponding to a self-defocusing nonlinearity.

To more clearly illustrate the main soliton features, we show typical stable and unstable cases of solitons propagation for different depths p of the periodic modulation of the Kerr nonlinearity. Their field profiles and their corresponding longitudinal evolutions are shown in Fig. 7. We find that regardless of the value of p , in the low power regime, the solitons have a multi-peaked light intensity distribution and exhibit stable propagation, while in high power regime, the corresponding light intensity has only one peak and the solitons exhibit unstable longitudinal evolution.

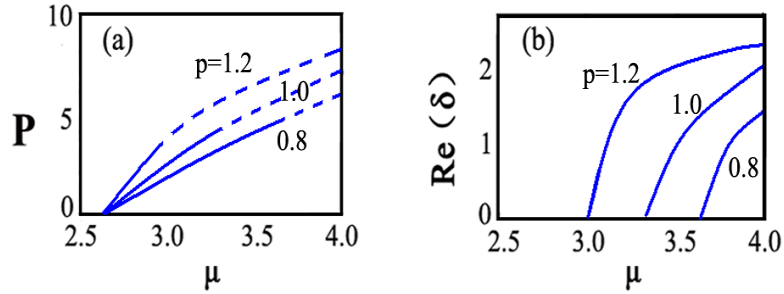


Fig. 6 – a) Power P versus μ ; b) $\text{Re}(\delta)$ versus μ for $\varepsilon = 4$ and $\omega_0 = 0.8$. The nonlinear modulation function is $N(x) = p \cos^2(2x)$ for $p = 1.2$, $p = 1$, and $p = 0.8$. The stable branches in panel (a) are plotted by solid curves and the corresponding unstable branches are plotted by dashed curves; after Ref. [43].

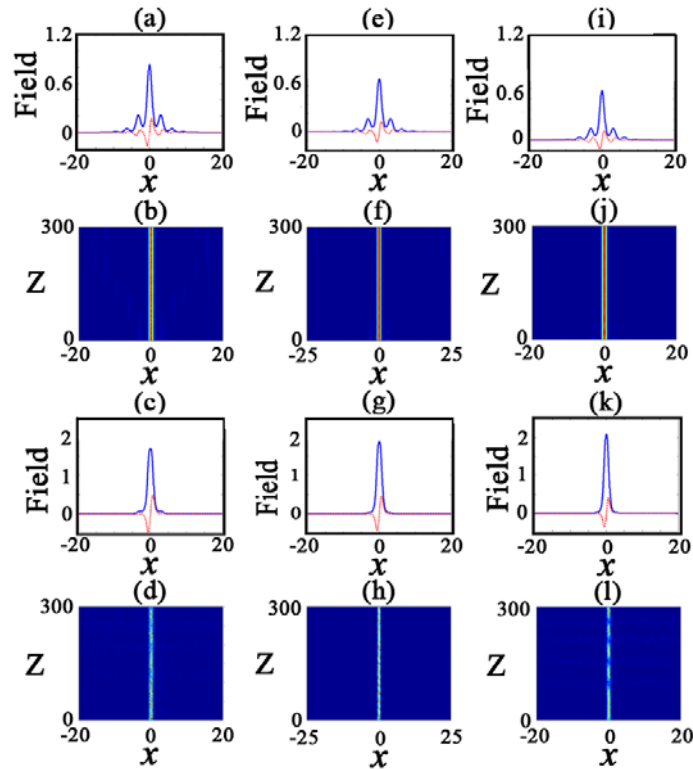


Fig. 7 – Soliton field profiles (the solid curves are for the real parts of the field profiles, whereas the dashed curves are for the imaginary parts of the field profiles), and the corresponding soliton propagation. For $p = 1.2$, the stable case is shown in (a, b) for $\mu = 2.7$, whereas the unstable case is shown in (c, d) for $\mu = 3.1$; for $p = 1$, the stable case is shown in (e, f) for $\mu = 2.7$, whereas the unstable case is shown in (g, h) for $\mu = 3.5$; for $p = 0.8$, the stable case is shown in (i, j) for $\mu = 2.7$, whereas the unstable case is shown in (k, l) for $\mu = 4.0$. The other parameters and the nonlinear modulation function are the same as in Fig. 6; after Ref. [43].

Note that in Ref. [43], it was studied the existence and stability of solitons in PT-symmetric periodic OLs only in the case of spatially periodic modulation of nonlinearities, unlike the previous work (see Ref. [44]) with PT-symmetric mixed linear-nonlinear OLs. Thus in Ref. [43] the space of free parameters of the problem was greatly reduced. Moreover, in that work, the strength p of the amplitude of the nonlinear modulation was considered for both self-focusing nonlinearities ($p \leq 1$) and for self-defocusing nonlinearities ($p > 1$). We end this section by noting that some of the results reported in Ref. [43] are different from those obtained for (a) PT-symmetric linear OLs [7,16], (b) PT-symmetric nonlinear OLs [35,42], and (c) PT-symmetric mixed linear-nonlinear OLs [44].

6. CONCLUSIONS

In this work we provided a brief overview of recent theoretical studies of optical spatial solitons in PT-symmetric mixed linear-nonlinear lattices. These nonlinear localized states are formed due to action of a confining potential representing a mixture of linear and nonlinear optical lattices. The linear optical lattices were considered to be either regular ones or superlattices. The latter are formed by the superposition of two periodic lattice potentials having commensurable periods. The results overviewed in this paper clearly show that different kinds of linear optical lattices can profoundly affect the unique spatial soliton properties.

A natural extension suggested by these studies is to consider the realistic situations of two- and three-dimensional optical systems. The results overviewed in the present work may find potential applications in the area of controlling or routing light in all-optical signal processing devices, and may be extended to other dissipative nonlinear systems with complex-valued external potentials [27,48-49].

Acknowledgements. This work was supported by the National Natural Science Foundation of China (Grant No. 11174061) and the Guangdong Province Natural Science Foundation of China (Grant No. S2011010005471). The work of D. M. was supported by CNCS-UEFISCDI, project number PN-II-ID-PCE-2011-3-0083.

REFERENCES

1. C. M. Bender, S. Boettcher, Phys. Rev. Lett., **80**, 5243 (1998).
2. Z. Ahmed, Phys. Lett. A, **282**, 343 (2001).
3. C. M. Bender, D. C. Brody, H. F. Jones, Phys. Rev. Lett., **89**, 270401 (2002).
4. C. M. Bender, D. C. Brody, H. F. Jones, Am. J. Phys., **71**, 1095 (2003).
5. C. M. Bender, D. C. Brody, H. F. Jones, B. K. Meister, Phys. Rev. Lett., **98**, 040403 (2007).

6. C. E. Rüter, K. G. Makris, R. El-Ganainy, D. N. Christodoulides, M. Segev, D. Kip, *Nat. Phys.*, **6**, 192 (2010).
7. Z. H. Musslimani, K. G. Makris, R. El-Ganainy, D. N. Christodoulides, *Phys. Rev. Lett.*, **100**, 030402 (2008).
8. K. G. Makris, R. El-Ganainy, D. N. Christodoulides, Z. H. Musslimani, *Phys. Rev. Lett.*, **100**, 103904 (2008).
9. K. G. Makris, R. El-Ganainy, D. N. Christodoulides, Z. H. Musslimani, *Phys. Rev. A*, **81**, 063807 (2010).
10. O. Bendix, R. Fleischmann, T. Kottos, B. Shapiro, *Phys. Rev. Lett.*, **103**, 030402 (2009).
11. H. Wang, J. Wang, *Opt. Express*, **19**, 4030 (2011).
12. K. Zhou, Z. Guo, J. Wang, S. Liu, *Opt. Lett.*, **35**, 2928 (2010).
13. X. Zhu, H. Wang, L.-X. Zheng, H. Li, Y.-J. He, *Opt. Lett.*, **36**, 2680 (2011).
14. Z. Shi, X. Jiang, X. Zhu, H. Li, *Phys. Rev. A*, **84**, 053855 (2011).
15. H. Li, Z. Shi, X. Jiang, X. Zhu, *Opt. Lett.*, **36**, 3290 (2011).
16. S. Nixon, L. Ge, J. Yang, *Phys. Rev. A*, **85**, 023822 (2012).
17. J. Zeng, Y. Lan, *Phys. Rev. E*, **85**, 047601 (2012).
18. V. Achilleos, P. G. Kevrekidis, D. J. Frantzeskakis, R. Carretero-González, *Phys. Rev. A*, **86**, 013808 (2012).
19. D. A. Zezyulin, V. V. Konotop, *Phys. Rev. Lett.*, **108**, 213906 (2012).
20. N. V. Alexeeva, I. V. Barashenkov, A. A. Sukhorukov, Y. S. Kivshar, *Phys. Rev. A*, **85**, 063837 (2012).
21. L. Chen, R. Li, N. Yang, D. Chen, L. Li, *Proc. Romanian Acad. A*, **13**, 46 (2012).
22. S. Liu, C. Ma, Y. Zhang, K. Lu, *Opt. Commun.*, **285**, 1934 (2012).
23. C. Li, H. Liu, L. Dong, *Opt. Express*, **20**, 16823 (2012).
24. S. Hu, X. Ma, D. Lu, Y. Zheng, W. Hu, *Phys. Rev. A*, **85**, 043826 (2012).
25. C. Yin, Y. He, Huagang Li, J. Xie, *Opt. Express*, **20**, 19355 (2012).
26. F. Lederer, G. I. Stegeman, D. N. Christodoulides, G. Assanto, M. Segev, Y. Silberberg, *Phys. Rep.*, **463**, 1 (2008);
D. Mihalache, D. Mazilu, F. Lederer, Y. S. Kivshar, *Opt. Lett.*, **32**, 3173 (2007);
Y. V. Kartashov, V. A. Vysloukh, D. Mihalache, L. Torner, *Opt. Lett.*, **31**, 2329 (2006);
D. Mihalache, M. Bertolotti, C. Sibilila, *Prog. Opt.*, **27**, 229 (1989);
D. Mihalache *et al.*, *Physica Scripta*, **29**, 269 (1984);
V. K. Fedyanin, D. Mihalache, *Z. Phys. B*, **47**, 167 (1982).
27. C.-K. Lam, B. A. Malomed, K. W. Chow, P. K. A. Wai, *Eur. Phys. J. Special Topics*, **173**, 233 (2009).
28. F. K. Abdullaev, V. V. Konotop, M. Salerno, A. Yulin, *Phys. Rev. E*, **82**, 056606 (2010).
29. Y. V. Kartashov, V. V. Konotop, V. A. Vysloukh, L. Torner, *Opt. Lett.*, **35**, 1638 (2010).
30. Y. V. Bludov, V. V. Konotop, *Phys. Rev. A*, **81**, 013625 (2010).
31. Y. V. Kartashov, V. V. Konotop, V. A. Vysloukh, *Europhys. Lett.*, **91**, 34003 (2010).
32. Y. He, D. Mihalache, X. Zhu, L. Guo, Y. V. Kartashov, *Opt. Lett.* **37**, 2526 (2012).
33. Y. V. Kartashov, B. A. Malomed, L. Torner, *Rev. Mod. Phys.*, **83**, 247 (2011).
34. S. V. Dmitriev, A. A. Sukhorukov, Y. S. Kivshar, *Opt. Lett.*, **35**, 2976 (2010).
35. F. K. Abdullaev, Y. V. Kartashov, V. V. Konotop, D. A. Zezyulin, *Phys. Rev. A*, **83**, 041805 (2011).
36. A. E. Miroshnichenko, B. A. Malomed, Y. S. Kivshar, *Phys. Rev. A*, **84**, 012123 (2011).
37. S. V. Suchkov, B. A. Malomed, S. V. Dmitriev, Y. S. Kivshar, *Phys. Rev. E*, **84**, 046609 (2011).
38. R. Driben, B. A. Malomed, *Opt. Lett.*, **36**, 4323 (2011).
39. R. Driben, B. A. Malomed, *Europhys. Lett.*, **96**, 51001 (2011).
40. Y. V. Bludov, V. V. Konotop, *Phys. Rev. A*, **74**, 043616 (2006).
41. F. Abdullaev, A. Abdumalikov, R. Galimzyanov, *Phys. Lett. A*, **367**, 149 (2007).

42. D. A. Zezyulin, Y. V. Kartashov, V. V. Konotop, *Europhys. Lett.*, **96**, 64003 (2011).
43. Y. He, X. Zhu, D. Mihalache, J. Liu, Z. Chen, *Opt. Commun.*, **285**, 3320 (2012).
44. Y. He, X. Zhu, D. Mihalache, J. Liu, Z. Chen, *Phys. Rev. A*, **85**, 013831 (2012).
45. J. Yang, *J. Computational Phys.*, **227**, 6862 (2008).
46. J. Yang, T. I. Lakoba, *Stud. Appl. Math.*, **118**, 153 (2007).
47. M. J. Ablowitz, Z. H. Musslimani, *Opt. Lett.*, **30**, 2140 (2005).
48. D. Mihalache, *Proc. Romanian Acad. A*, **11**, 142 (2010); D. Mihalache, *Rom. J. Phys.*, **57**, 352 (2012).
49. D. Mihalache, D. Mazilu, *Rom. Rep. Phys.*, **60**, 749 (2008);
D. Mihalache, *Rom. Rep. Phys.*, **63**, 9 (2011); D. Mihalache, *Rom. Rep. Phys.*, **63**, 325 (2011).